

Mixed Convection in a Lid-Driven Square Cavity With Heat Sources Using Nanofluids

Ilhem Zeghbid¹ and Rachid Bessaïh¹

Abstract: This paper presents a numerical study of two-dimensional laminar mixed convection in a lid-driven square cavity filled with a nanofluid and heated simultaneously at a constant heat flux q'' by two heat sources placed on the two vertical walls. The movable wall and the bottom wall of the cavity are maintained at a local cold temperature T_c , respectively. The finite volume method was used to solve the equations of flow with heat transfer across the physical domain. Comparisons with previous results were performed and found to be in excellent agreement. Results were presented in terms of streamlines, isotherms, vertical velocity profile, and local and average Nusselt numbers for Rayleigh number in the range ($Ra=10^3-10^6$), Reynolds number ($Re=1-500$), solid volume fraction of nanoparticles ($\phi=0-0.10$), heat sources locations, and type of nanofluids (Cu, Ag, Al_2O_3 and TiO_2). The influence of the relevant parameters such as the Rayleigh number, the Reynolds number and the volume fraction of the nonofluid on the average Nusselt number was studied in detail. It was found that the average Nusselt number increases with the increase of Rayleigh number and solid volume fraction of nanofluids. The results show that the Cu-water nanofluid improves heat transfer, and that the heat sources position has an influence on the flow and thermal fields, and on the local and average Nusselt numbers.

Keywords: Mixed convection, heat sources, cavity, nanofluids.

Nomenclature

¹ University Constantine 1, Department of Mechanical Engineering, LEAP Laboratory, Route de Ain El. Bey, Constantine 25000, ALGERIA.

Email: leap.mechanical@gmail.com; Phone/Fax: +213 31 81 88 96.

b	length of heat source, m	x, y	horizontal and vertical coordinates, m
B	dimensionless length of the heat source (b/L)	X, Y	dimensionless horizontal and vertical coordinates (x/L, y/L)
d	distance of heat source, m	ΔT	temperature difference ($q''L/k_f$)
D	dimensionless distance of the heat source (d/L)	T	temperature, K
C_p	specific heat, $\text{JKg}^{-1} \text{K}^{-1}$	Greek symbols	
g	acceleration of gravity, ms^{-2}	ψ	dimensionless stream function
L	length of the cavity, m	ϕ	solid volume fraction
k	thermal conductivity, $\text{Wm}^{-1}\text{K}^{-1}$	θ	dimensionless temperature
Nus	local Nusselt number on the heat source surface	ν	kinematic viscosity, m^2s^{-1}
\overline{Nu}	average Nusselt number along the heat source	μ	dynamic viscosity, $\text{kg m}^{-1}\text{s}^{-1}$
p	pressure, Pa	ρ	density, $\text{kg}\cdot\text{m}^{-3}$
P	dimensionless pressure ($p/p_{nf} U_0^2$)	α	thermal diffusivity, $\text{m}^2 \text{s}^{-1}$
Pr	Prandtl number (ν_f/α_f)	β	thermal expansion coefficient, K^{-1}
q''	heat flux per area, Wm^{-2}	Subscripts	
Ra	Rayleigh number ($g \beta_f L^3 \Delta T/\nu_f \alpha_f$)	c	cold wall
Re	Reynolds number ($Re=\rho_f U_0 L/\mu_f$)	nf	nanofluid
U, V	dimensionless horizontal and vertical velocity components	s	solid
u, v	horizontal and vertical velocity components, ms^{-1}	f	pure fluid
U_0	velocity, ms^{-1}	p	nanoparticle
t	time, s	m	average
		TT	Top-Top
		MM	Midle-Midle
		DD	Down-Down
		TD	Top-Down

1 Introduction

Nanofluids are dispersions of nano-sized particles (having a diameter typically less than 100 nm), called nanoparticles in a basic medium in order to improve certain properties. In the case of heat transfer fluids, one of the first parameters to be taken into account to evaluate the potential for heat exchange is the thermal conductivity. However, the most widely used fluids, such as water, oil or ethylene glycol (EG) have only a low thermal conductivity compared to that of crystalline solids. With nanofluids, the idea is to insert the nanoparticles in the base fluid in order to increase the effective thermal conductivity of the mixture. Choi [Choi (1995)] introduced the term nanofluid in 1985. Because of their

excellent thermal performance, the examples relate to heat exchangers, microchannels, cooling of electronic systems, nuclear reactors, buildings, grain storage, etc. Some works are described briefly, as follows.

Rahman et al. [Rahman, Billah, Hasanezzaman et al. (2012)], Talebi et al. [Talebi, Mahmoudi and Shahi (2010)], and Pourmahmoud et al. [Talebi, Mahmoudi and Shahi (2013)] showed that the nanoparticles have a major influence on the flow and thermal fields. Mansour et al. [Mansour, Shahi and Talebi (2010)] found that the type of nanofluids is a key factor for improving transfer, and the highest values were observed when they used copper as nanoparticle. Salari et al. [Salari, Tabar, Tabar et al. (2012)] presented the results of a numerical study of mixed convection within a fluid cavity filled with a nanofluid. The results show that the heat transfer increases with an increase in the Rayleigh, while it decreases with increasing volume fraction of the nanoparticle and the Reynolds number. Abu-Nada et al. [Abu-Nada and Chamkha (2010)] numerically studied laminar mixed convection flow in a lid-driven inclined square enclosure filled with a nanofluid. The results show that significant improvement of heat transfer could be obtained due to the presence of nanoparticles and the inclination of the enclosure. Mahmoudi et al. [Mahmoudi, Shahi, Shahedin et al. (2011)] conducted a computer simulation on the natural convection cooling in an open cavity subjected to nanofluid (Cu-water). The results indicate that the average Nusselt number is an increasing function of the concentration of nanoparticles. Sebdania et al. [Sebdania, Mahmoodia, Hashemi (2012)] performed a numerical study of mixed convection in a square cavity filled with a nanofluid. The results show that when the heat source is in the middle, the effect of the addition of nanoparticles increases with increasing the Reynolds number, and that the transfer rate is decreased with increasing the solid volume fraction of nanoparticles.

Alinia et al. [Alinia, Ganji and Gorji-Bandpy (2011)] exhibited the thermal behaviour of a nanofluid (SiO₂-water) for different inclination angles of an inclined two-sided lid-driven cavity using two-phase mixture model. They found that the concentration (SiO₂) nanoparticles remarkably increase the heat transfer rate. Khorasanizadeh et al. [Khorasanizadeh, Nikfar and Amani (2013)] studied the mixed convection and entropy generating of Cu-water nanofluid in a square cavity with an active lid. The results show that the addition of nanoparticles to the base fluid affects the entropy generation. Akbari et al. [Akbari, Behzadmehr and Shahraki (2008)] made a numerical simulation of mixed convection in horizontal and inclined tubes with uniform heat flux using a nanofluid. The results show that the concentration of Al₂O₃ is not significant effects on hydrodynamic parameters, and that the heat transfer coefficient is maximum when the angle of inclination is equal to 45°. Jmai et al. [Jmai, Ben-Beya and Lili (2013)] and Mahmoudi et al. [Mahmoudi and Hashemi (2012)] examined the effects of parameters such as the Rayleigh number, the solid volume fraction of nanoparticles and the heat sources locations on the natural convection flow in a partially heated cavity filled with different types of nanoparticles (Cu, Ag, Al₂O₃ and TiO₂). They found that the heat transfer increases with the increasing of Rayleigh number and concentration of the nanoparticle, and the Cu-water nanofluid ensures a very high transfer versus nanofluids (water-Al₂O₃ and water-TiO₂). Arami et al. [Arami, Sebdani and Mahmoudi (2012)] dealt with the phenomenon of the sinusoidal heating side of a cavity filled with a nanofluid. The results show that the heat transfer rate increases with the decrease in Richardson and increasing the concentration of

nanoparticles. Nasrin et al. [Nasrin, Alim and Chamkha (2012)] focused on the numerical modelling of laminar mixed convection flow in a wavy triangular cavity filled with a nanofluid.

Pishkar Pishkar and Ghasemi [Pishkar and Ghasemi (2012)] showed a numerical study on thermal performance through two fins mounted on a horizontal channel with a fluid cooled and Cu-water nanofluid. The results found show that the influence of the concentration of nanoparticles on heat transfer is more apparent at higher values of the Reynolds number. Shariat et al. [Shariat, Akbarinia, Nezhad et al. (2011)] numerically studied the mixed convection of a nanofluid in elliptical pipes. Brownian motion of nanoparticles was considered for the determination of thermal conductivity and dynamic viscosity of the nanofluid. Mansour et al. [Mansour, Galanis and Nguyen (2011)] conducted an experimental study of mixed convection with a nanofluid in an inclined tube with uniform wall heat flux. Soleimani et al. [Soleimani, Oleslani, Ganji et al. (2012)], Mahmoudi and Sebdani [Mahmoudi and Sebdani (2012)], and Akbarinia and Behzadmehr [Akbarinia and Behzadmehr (2007)] numerically studied natural convection in a semi-annular cavity filled with a nanofluid. Mahmoudi et al. [Mahmoudi, Shahi, Shahedin et al. (2011)] made a numerical simulation of natural convection in a square cavity with a thin inside the heater. The results show that at high Rayleigh numbers, the Ag-water nanofluid is more effective to increase the heat transfer rate, while for low Rayleigh numbers the type of nanofluid does not affect the heat transfer. Shahi et al. [Shahi, Mahmoudi and Talebi (2010)] numerically investigated mixed convection cooling in a square cavity ventilated and partially heated from the below utilizing nanofluid. Mahmoudi et al. [Mahmoudi, Shahi and Talebi (2010)] numerically studied the effect on inlet and outlet location on the mixed convection cooling inside the ventiled cavity subjected to an external nanofluid. The authors noted that the presence of the nanoparticle is more effective in Top-Down configuration, while increasing the concentration of the nanoparticle has the least effect in the Top-Top configuration. Haddad et al. [Haddad, Oztop, Abu-Nada et al. (2012)] presented an overview of various recent experimental and theoretical studies to examine and explain the reasons for improved heat transfer in natural convection with nanofluid models. The literature review indicates that most of the numerical results show that nanofluids significantly improve the ability of heat transport.

The objective of this study is to investigate the mixed convection in a lid-driven square cavity filled with a nanofluid and heated simultaneously at a constant heat flux q'' by two heat sources placed on the two vertical walls. The influence of relevant parameters such as the Rayleigh and Reynolds numbers, solid volume fraction, type of nanofluids and heat sources locations on the local and average Nusselt numbers were studied in detail. This geometry has potential application in the cooling of electronic components.

This paper is organized as follows. Section 2 presents the geometry and mathematical model with boundary conditions. Section 3 discusses the numerical method and code validation. Section 4 presents the results and discussion. Finally, a conclusion is given.

2 Geomety and mathematical model

2.1 Geometry

The geometries considered in this study are illustrated in Figure 1. A square cavity of dimensions L is filled with a nanofluid. A two identical heat sources with constant heat flux q'' of dimension b are placed on the vertical walls of the cavity. The top and bottom walls are maintained at a local cold temperature T_c , while the top wall moved with uniform velocity of U_0 . The remaining boundaries on the vertical walls are adiabatic. The four configurations are namely Middle-Middle (MM), Top-Top (TT), Down-Down (DD) and Top-Down (TD).

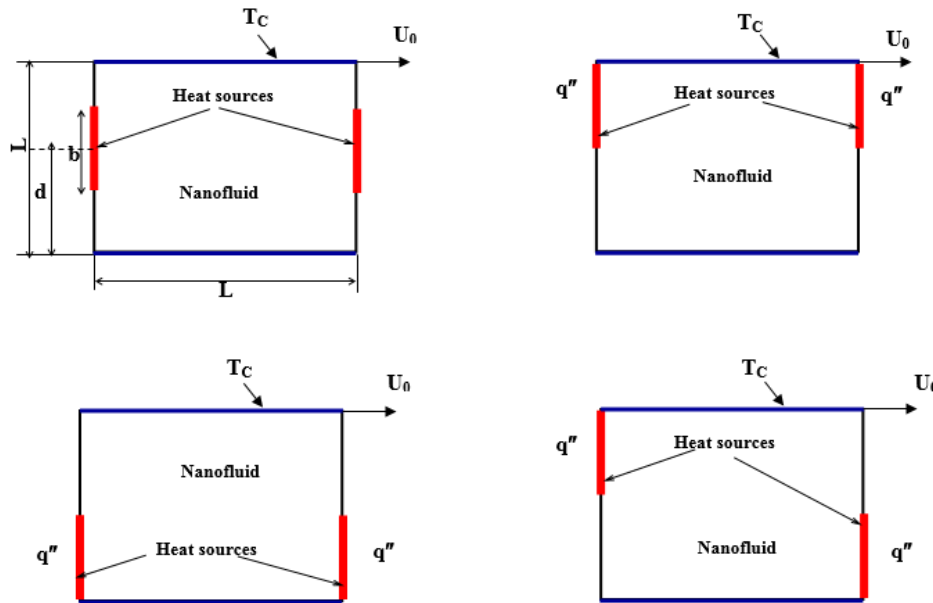


Figure 1: A schematic diagram of the physical model and boundary conditions for a lid-driven square cavity: (a) case MM (Middle-Middle), (b) case TT (Top-Top), (c) case DD (Down-Down) and (d) case TD (Top-Down)

2.2 Governing Equations

The thermo-physical properties of the nanofluid are considered constant except for the density variation with temperature in the buoyancy force of the Y-momentum equation (Boussinesq's hypothesis). The nanofluids are assumed Newtonian, incompressible, and laminar. The nanoparticles are assumed to have uniform shape and size, and in a thermal equilibrium state with the base fluid. Table 1 presents the thermo-physical properties of nanoparticles (Cu, Ag, Al_2O_3 and TiO_2) and the base fluid (pure water). The equations of continuity, momentum and energy with the above assumptions can be written as follows.

Table 1: Thermo-physical properties of water, silver, copper, alumina and titanium

	ρ (kg·m ⁻³)	β (K ⁻¹)	k (W m ⁻¹ K ⁻¹)	C_p (J kg ⁻¹ K ⁻¹)
Pure water	997.1	21×10^{-5}	0.613	4179
Silver (Ag)	10500	1.89×10^{-5}	429	235
Copper (Cu)	8933	1.67×10^{-5}	401	385
Alumina (Al ₂ O ₃)	3970	0.85×10^{-5}	40	3970
Titaniumn (TiO ₂)	4250	0.9×10^{-5}	8.9538	686.2

$$\frac{\partial u}{\partial x} + \frac{\partial v}{\partial y} = 0 \quad (1)$$

$$u \frac{\partial u}{\partial x} + v \frac{\partial u}{\partial y} = \frac{1}{\rho_{nf}} \left[-\frac{\partial p}{\partial x} + \mu_{nf} \left(\frac{\partial^2 u}{\partial x^2} + \frac{\partial^2 u}{\partial y^2} \right) \right] \quad (2)$$

$$u \frac{\partial v}{\partial x} + v \frac{\partial v}{\partial y} = \frac{1}{\rho_{nf}} \left[-\frac{\partial p}{\partial y} + \mu_{nf} \left(\frac{\partial^2 v}{\partial x^2} + \frac{\partial^2 v}{\partial y^2} \right) \right] + (\rho\beta)_{nf} g(T - T_c) \quad (3)$$

$$u \frac{\partial T}{\partial x} + v \frac{\partial T}{\partial y} = \alpha_{nf} \left(\frac{\partial^2 T}{\partial x^2} + \frac{\partial^2 T}{\partial y^2} \right) \quad (4)$$

where u and v are the horizontal and vertical velocity components, respectively; p is the pressure and T is the temperature.

The effective density of the nanofluid at the reference temperature can be defined as

$$\rho_{nf} = (1-\phi)\rho_f + \phi\rho_p \quad (5)$$

The thermal expansion coefficient of the nanofluid $(\rho\beta)_{nf}$ can be determined as

$$(\rho\beta)_{nf} = (1-\phi)(\rho\beta)_f + \phi(\rho\beta)_p \quad (6)$$

The thermal diffusivity of the nanofluid α_{nf} can be expressed by

$$\alpha_{nf} = \frac{k_{nf}}{(\rho c_p)_{nf}} \quad (7)$$

The heat capacitance of nanofluids can be determined by

$$(\rho c_p)_{nf} = (1-\phi)(\rho c_p)_f + \phi(\rho c_p)_p \quad (8)$$

The dynamic viscosity of nanofluid presented by Brinkman [Brinkman (1952)] is determined by the following.

$$\mu_{nf} = \frac{\mu_f}{(1-\phi)^{2.5}} \quad (9)$$

In this research, the thermal conductivity of nanofluids k_{nf} was taken to be similar to other

studies such as Rahman et al. [Rahman, Billah, Hasanezzaman et al. (2012)]; Mansour et al. [Mansour, Mohamed, Abdel-Elaziz et al. (2010)]; Salari et al. [Salari, Tabar, Tabar et al. (2012)]; Abu-Nada et al. [Abu-Nada and Chamkha (2010)] as follows.

$$k_{nf} = \frac{k_p + 2k_f - 2\phi(k_f - k_p)}{k_p + 2k_f + \phi(k_f - k_p)} k_f \quad (10)$$

where k_p is the thermal conductivity of dispersed nanoparticles, and k_f is the thermal conductivity of the pure fluid.

The governing equation are nondimensionlezed by using the following variables:

$$X=x/L, Y=y/L, U=u/U_0, V=v/U_0, P=p/\rho_{nf} U_0^2, \text{ and } \theta=T-T_C/\Delta T, \Delta T=q''L/k_f \quad (11)$$

The dimensionless equations governing the flow are written as follows.

$$\frac{\partial U}{\partial X} + \frac{\partial V}{\partial Y} = 0 \quad (12)$$

$$U \frac{\partial U}{\partial X} + V \frac{\partial U}{\partial Y} = -\frac{\partial P}{\partial X} + \frac{1}{\text{Re}} \frac{\rho_f}{\rho_{nf}} \frac{1}{(1-\phi)^{2.5}} \left[\frac{\partial^2 U}{\partial X^2} + \frac{\partial^2 U}{\partial Y^2} \right] \quad (13)$$

$$U \frac{\partial V}{\partial X} + V \frac{\partial V}{\partial Y} = -\frac{\partial P}{\partial Y} + \frac{1}{\text{Re}} \frac{\rho_f}{\rho_{nf}} \frac{1}{(1-\phi)^{2.5}} \left[\frac{\partial^2 V}{\partial X^2} + \frac{\partial^2 V}{\partial Y^2} \right] + \frac{(\rho\beta)_{nf}}{\rho_{nf} \beta_f} \frac{Ra}{\text{Pr Re}^2} \theta \quad (14)$$

$$U \frac{\partial \theta}{\partial X} + V \frac{\partial \theta}{\partial Y} = \frac{\alpha_{nf}}{\alpha_f} \frac{1}{\text{Re Pr}} \left[\frac{\partial^2 \theta}{\partial X^2} + \frac{\partial^2 \theta}{\partial Y^2} \right] \quad (15)$$

In Eq. (13)-(15), the non-dimensional parameters are the Reynolds number $Re=U_0L/\nu_f$, the Rayleigh number $Gr=g\beta_f\Delta TL^3/(\alpha_{nf})$, the Prandtl number $Pr=\nu_f/\alpha_f$, and ϕ the solid volume fraction of nanoparticles.

2.3 Boundary conditions

The boundary conditions are presented in dimensionless form, as follows:

- **At the vertical left wall:**

$$\text{For } X=0 \text{ and } 0 \leq Y \leq (D-0.5B): U=V=0, \frac{\partial \theta}{\partial X} = 0$$

$$\text{For } X=0 \text{ and } (D-0.5B) \leq Y \leq (D+0.5B): U=V=0, \frac{\partial \theta}{\partial X} = -\frac{k_f}{k_{nf}}$$

$$\text{For } X=0 \text{ and } (D+0.5B) \leq Y \leq 1: U=V=0, \frac{\partial \theta}{\partial X} = 0$$

- **At the vertical right wall:**

$$\text{For } X=1 \text{ and } 0 \leq Y \leq (D-0.5B): U=V=0, \frac{\partial \theta}{\partial X} = 0$$

$$\text{For } X=1 \text{ and } (D-0.5B) \leq Y \leq (D+0.5B): U=V=0, \frac{\partial \theta}{\partial X} = -\frac{k_f}{k_{nf}}$$

$$\text{For } X=1 \text{ and } (D+0.5B) \leq Y \leq 1: U=V=0, \frac{\partial \theta}{\partial X} = 0$$

- **At the bottom and top walls:**

$$\text{For } Y=0 \text{ and } 0 \leq X \leq 1: U=V=0, \theta=0$$

$$\text{For } Y=1 \text{ and } 0 \leq X \leq 1: U=1, V=0, \theta=0.$$

2.4 Local and average Nusselt numbers

The local Nusselt number on the heat source surface is defined as:

$$Nu = \frac{hL}{k_f} \quad (16)$$

where h is the heat transfer coefficient determined by:

$$h = \frac{q''}{T_s - T_c} \quad (17)$$

By using the dimensionless variables mentioned above, the local Nusselt number becomes:

$$Nu_s(Y) = \frac{1}{\theta_s(Y)} \quad (18)$$

where θ_s is the dimensionless heat source temperature. Finally, the average Nusselt number Nu_m along the heat source can be obtained as:

$$Nu_m = \frac{1}{B} \int_{D-0.5B}^{D+0.5B} Nu_s(Y) dY \quad (19)$$

Here, B ($=b/L$) and D ($=d/L$) are the dimensionless length and distance of the heat source, respectively.

3 Numerical method and code validation

3.1 Numerical method

The governing equations presented in Eq. (12)-(15) along with the boundary conditions were solved by using FORTRAN code, which using a control volume formulation [Patankar (1980)]. The numerical procedure called SIMPLER [Patankar (1980)] was used to handle the pressure-velocity coupling. For treatment of the convection and diffusion terms in Eq. (13)-(15), power-law scheme was adopted. The convergence was obtained when the energy balance between the heat sources and the cold wall is less than a prescribed accuracy value, i.e. 0.2%.

3.2 Grid independence study

A grid independency study was examined to ensure the accuracy and reliability of the numerical methods and to improve the accuracy of the simulation results. Six different mesh sizes were used: 42×42 , 62×62 , 82×82 , 102×102 , 122×82 , and 122×122 nodes. For each mesh size, table 2 presents the average Nusselt (Nu_m) and the dimensionless maximal temperature of the heat source $\theta_{s,max}$ for the MM case at $Ra=10^5$, Cu-water nanofluid, $Re=10$, and $\phi=0.10$. The results show that a grid size of 122×122 nodes satisfies the grid independence. This grid was therefore adopted for all numerical simulations.

Table 2: Grid Study results for a MM case ($Ra=10^5$, Cu-water, $Re=10$ and $\phi = 0.10$): Average Nusselt number along the hot wall and the maximum temperature heat source for different grids

Grid	42×42	62×62	82×82	102×102	122×122	142×142
Nu_m	6.9590	6.8800	6.8410	6.8180	6.8090	6.8080
$\theta_{s,max}$	0.1880	0.1860	0.1850	0.1840	0.1840	0.1840

3.3 Code validation

To verify the accuracy of the present numerical study, the code was validated with the numerical results of Salari et al. [Salari, Tabar, Tabar et al. (2012)], Abu-Nada et al. [Abu-Nada and Chamkha (2010)]. For Salari et al. [Salari, Tabar, Tabar et al. (2012)], a comparison of the dimensionless vertical velocity V with X for Cu-water nanofluid, Reynolds number, $Re=10$, Rayleigh numbers $Ra=10^3, 10^4, 10^5$, and two values of the solid volume fraction $\phi=0$ and 0.20 . For Abu-Nada and Chamkha [Abu-Nada and Chamkha (2010)], a comparison of the dimensionless temperature θ and the dimensionless horizontal velocity, U with Y for mixed convection flow in a lid-driven inclined square enclosure filled with a nanofluid. As shown in Figure 2a-b and 3a-b, it is clear that our results are in good agreement with the numerical results of Salari et al. [Salari et al. (2012)], and Abu-Nada and Chamkha [Abu-Nada and Chamkha (2010)].

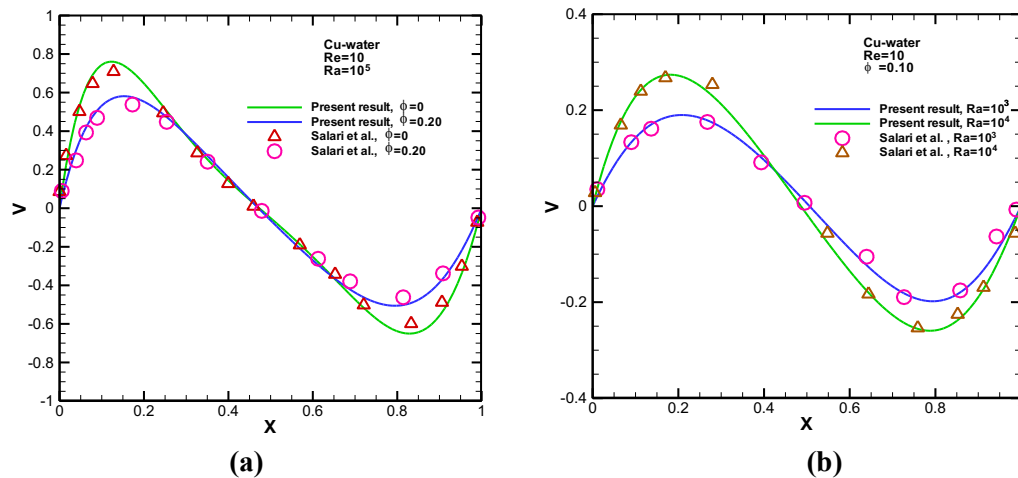


Figure 2: Validation of the present code with the numerical results of Salari et al. [Salari, Tabar, Tabar et al. (2012)] for the velocity profiles with X in the middle

section of the square cavity filled with Cu-water nanofluid: (a) at $Re=10$, $Ra=10^5$, $\phi=0$ and $\phi=0.20$, (b) at $Re=10$, $\phi=0.10$, $Ra=10^3$ and 10^4

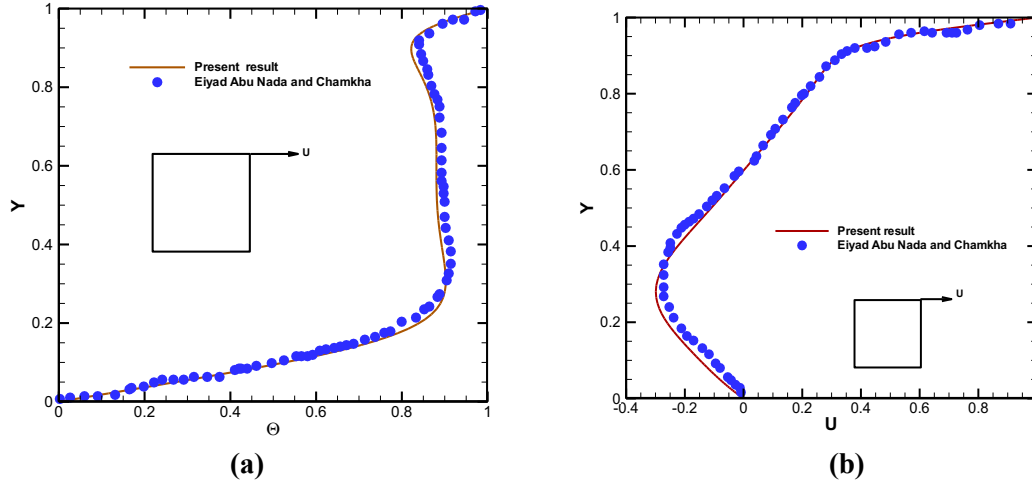


Figure 3: Validation of the present code with the numerical results of Abu-Nada and Chamkha [Abu-Nada and Chamkha (2010)] in the middle section of the square cavity at $Re=10$ and $Ra=10^5$: (a) for the dimensionless temperature profiles, (b) for the dimensionless horizontal velocity.

4 Results and discussion

The steady state results presented in this paper are generated for different parameters: Ra number ($Ra=10^3-10^6$), Reynolds number ($Re=1-500$), solid volume fraction of nanoparticles ($\phi=0-0.10$). The study deals with the effects of the Rayleigh and Reynolds numbers, solid volume fraction, type of nanofluids, and heat sources position on the flow structure, the temperature field, the variation of the vertical velocity V , and the local and average Nusselt numbers along the heat sources. The numerical results are presented in terms of streamlines, isotherms, local and average Nusselt numbers.

4.1 Effects of Rayleigh number

Figure 4 shows the streamlines (on the left) and isotherms (on the right) for the lid-driven square cavity with Cu-water nanofluid ($\phi=0.10$) at different Rayleigh numbers and $Re=10$. For $Ra=10^3$ and 10^4 (Figure 4a and 4b), we can see a rotary movement within the chamber through a cell provided with a recirculation in the upper part of the cavity near the movable wall. By increasing the Rayleigh number, the flow pattern is composed of two cells turn the opposite direction, the size of the recirculation zones increases. This is due to the increase in Rayleigh number. This increase in the size of the recirculation zone counterclockwise serves to release the heat to the flow of the main fluid. While the recirculation zone and a dead zone is isolated from the main fluid flow, but this counterclockwise recirculation zone helps to cool the cavity. We note that the temperature gradients are quite large in the vicinity of the active sources, against stratification is observed near the horizontal walls, the important thermal stratification leads the liquid to

become cooler, which considerably improves the cooling of the cavity. For high Rayleigh number $Ra=10^5$ and 10^6 (Figure 4c and 4d), it is interesting to indicate that the buoyancy forces are not negligible, hence the continued existence of recirculation zones, an asymmetric behavior is presented the middle plane of the cavity. This asymmetry is accompanied by an increase in the intensity of the flow through the increase of the streamlines. It is clear from the obtained isotherms are affected by the location of the two heat sources and the movement of the upper wall in the horizontal plane. The results for pure water ($\phi=0$) are also shown in Figure 4a, 4b, 4c, and 4d, it is also clear that when nanofluid is added, the maximum dimensionless temperature experienced a reduction; it is an indication of improved cooling performance of the cavity.

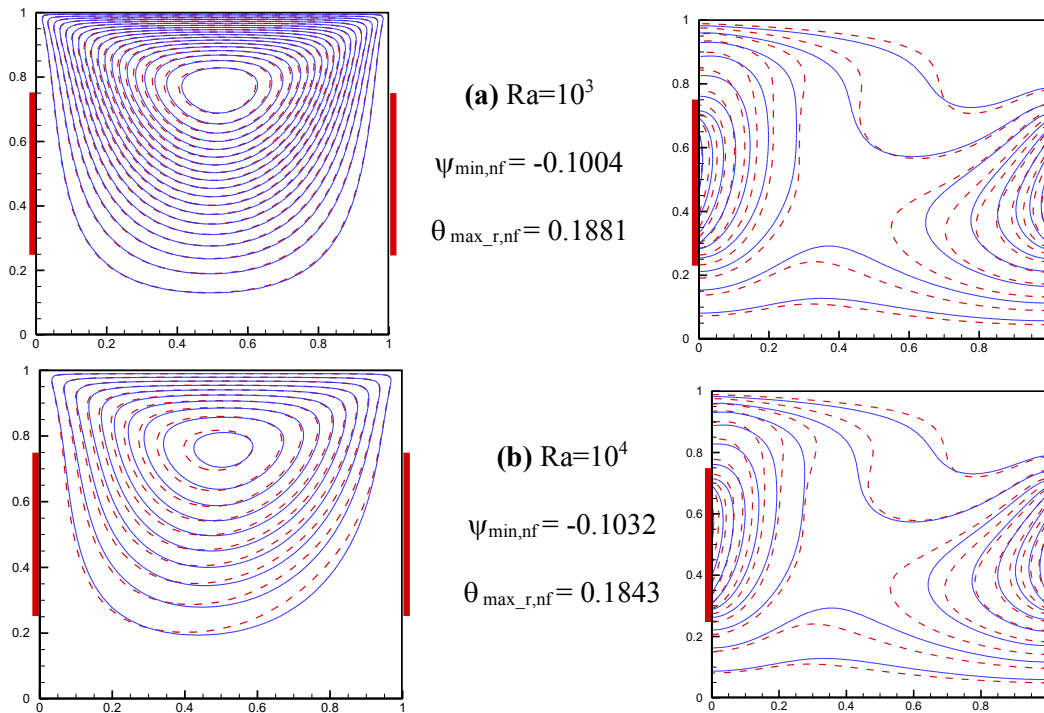


Figure 4: Streamlines (on the left) and isotherms (on the right) for different values of Rayleigh number for the lid-driven cavities filled with Cu-water nanofluid, $\phi=0.10$ (—), and pure water $\phi=0$ (---) at $Re=10$. (a) $Ra=10^3$, (b) $Ra=10^4$ (c) $Ra=10^5$ (d) $Ra=10^6$

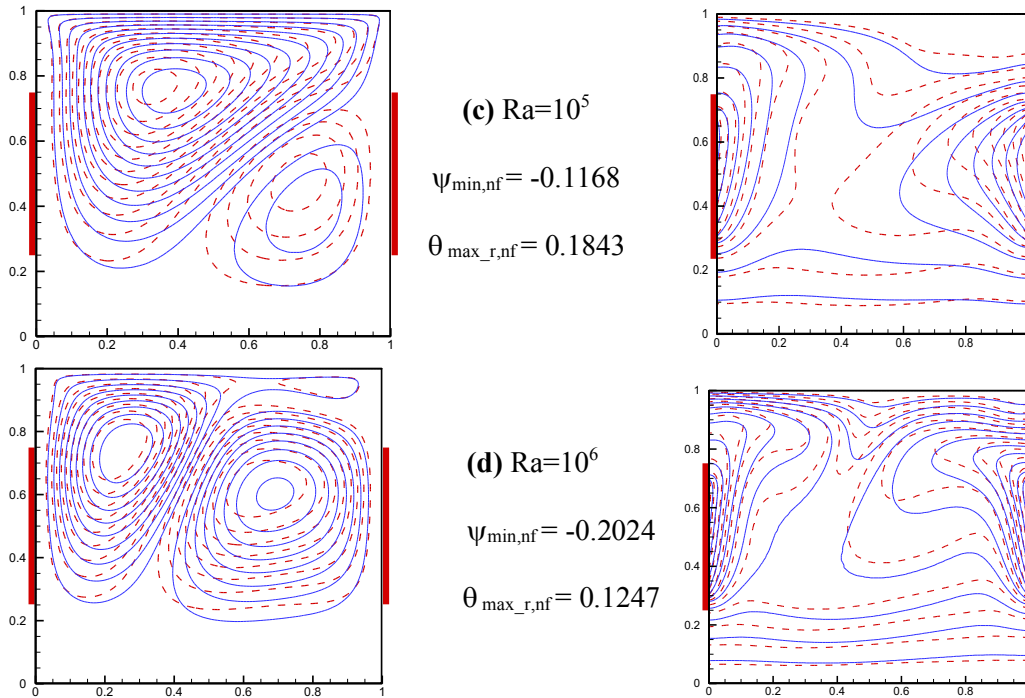
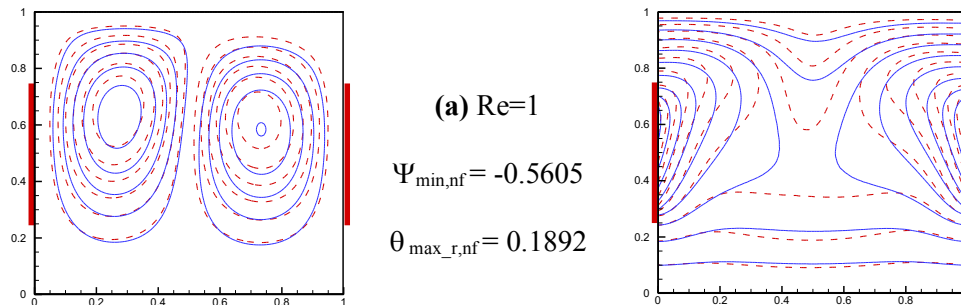


Figure 4 (continued)

4.2 Effects of Reynolds number

Figure 5 shows the effect of Reynolds number Re on the streamlines (on the left) and isotherms (on the right) for different values of Re for the lid-driven cavities filled with Cu-water nanofluid at $Ra=10^5$. We note that while increasing the Reynolds number, the effect of the cover rises due to forced convection, and for high values of Reynolds number ($Re=500$, Figure 5e), it was observed that the presence of heat sources has not a visible effect on the streamlines. In addition, the movement of fluid in the upper part of the cavity and the movement of the lid generated a range of current lines to the left wall of the cavity. The distribution of isothermal contours within the cavity for lower Reynolds numbers ($Re=1$, Figure 5a) gives a maximum temperature $\theta_{\max}=0.1892$. For Reynolds numbers $Re=10$, 50, 100, and 500, the fluid temperature decreases and nano isothermal contours focus to the left sidewall. This behaviour is clearly shown in Figure 5.



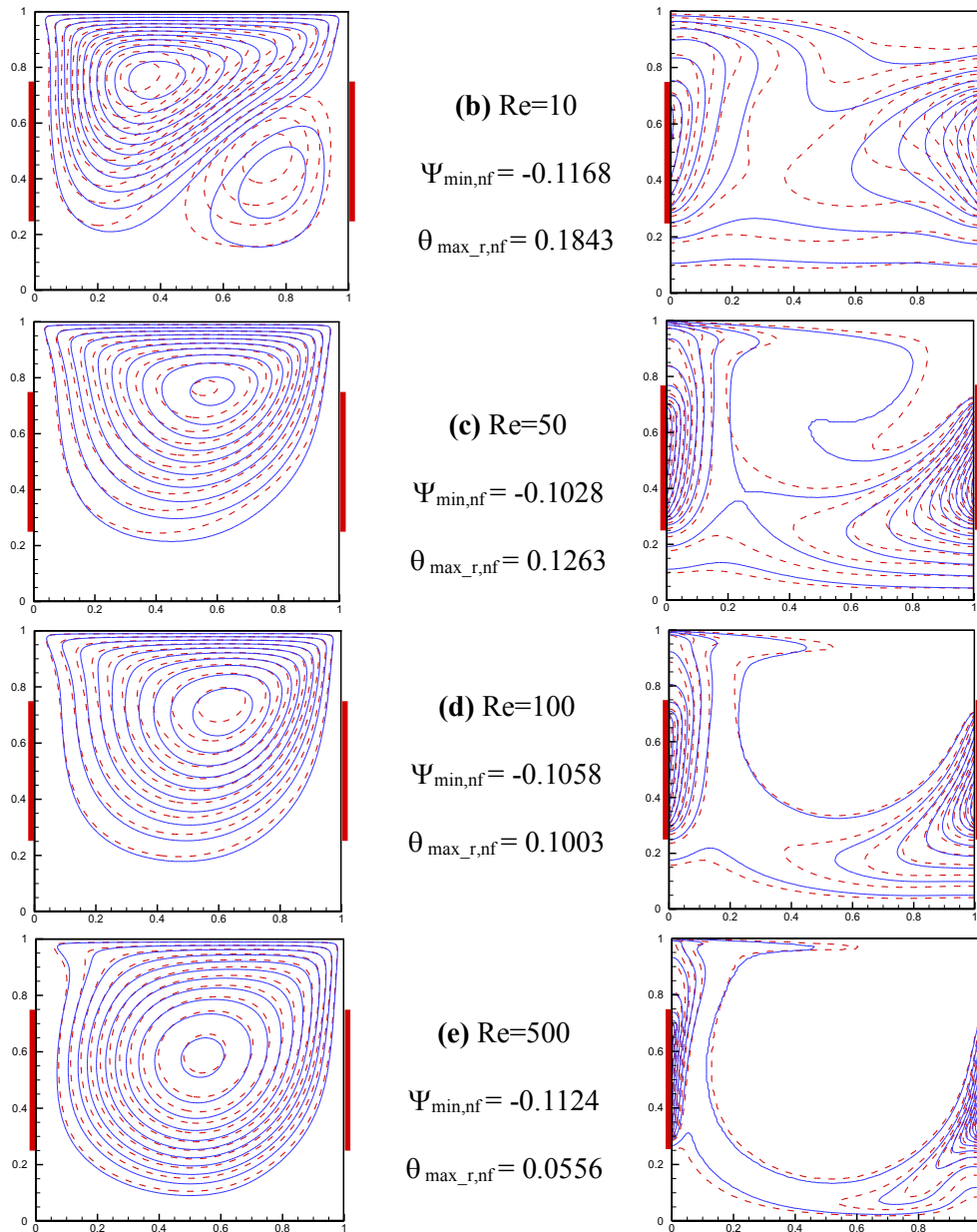
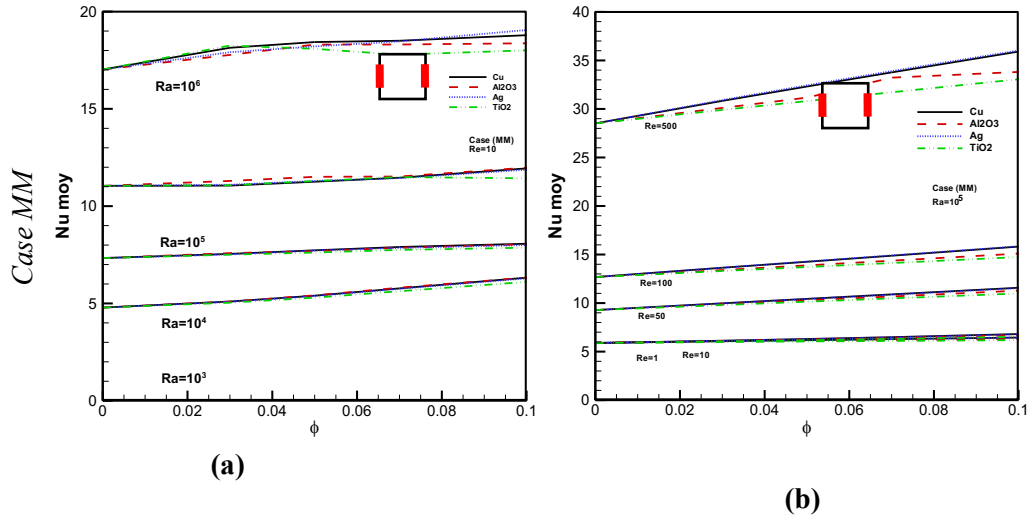


Figure 5: Streamlines (on the left) and isotherms (on the right) for different values of Reynolds number for the lid-driven cavities filled with Cu-water nanofluid, $\phi=0.10$ (—), and pure water $\phi=0$ (---) at $Ra=10^5$. (a) Re=1, (b) Re=10 (c) Re=50 (d) Re=100, (e) Re=500

4.3 Effects of nanofluids

In order to examine the effect of nanofluids on the average Nusselt number Nu_m , simulations were performed for various Rayleigh and Reynolds numbers. Figures 6a-6h

show the variation of the average Nusselt number Nu_m along the heat source with solid volume fraction at various Rayleigh and Reynolds numbers and different nanofluids (Cu-water, Al_2O_3 -water, Ag-water, TiO_2 -water) and heat sources locations. It was noticed when increasing the Rayleigh number, the average Nusselt number increases, showing the significant effect of the Rayleigh number on the transfer rate within the cavity. Furthermore, it was observed that the largest number average Nusselt values were detected in the DD case. This is mainly due to the large temperature gradient exists within the cavity above the locality of two heat sources, which is very far compared to the cold top wall. Also, it was found that increasing the average Nusselt number for different locations of heat sources for $Ra=10^6$ is about 24.42% for MM case, 24.88 % for TT case, 25.57% for DD case, and 25.11% for cross- location TD. According to these features of the above data, we appreciate the role of the heat source location in increasing the rate of removal of the heat and the type of the nanofluid. More heat transfer is obtained for Cu-water nanofluid and DD case. Figures 6b-h expose the distribution of average Nusselt number as a function of the Reynolds number for a square cavity filled with different nanofluids. We can see that the average Nusselt number increases while increasing the Reynolds number. It was found that for nanofluids (Cu-water) or (water-Ag) and for the location near the upper cold wall, the average Nusselt number reaches large values of the order of 26.21% for the mid- section location (MM), 38.10% for TT case, 16.34% for DD case, and 19.32% for TD case. It can be concluded that the Nusselt number of two heat sources increases with increase in Rayleigh and Reynolds numbers.



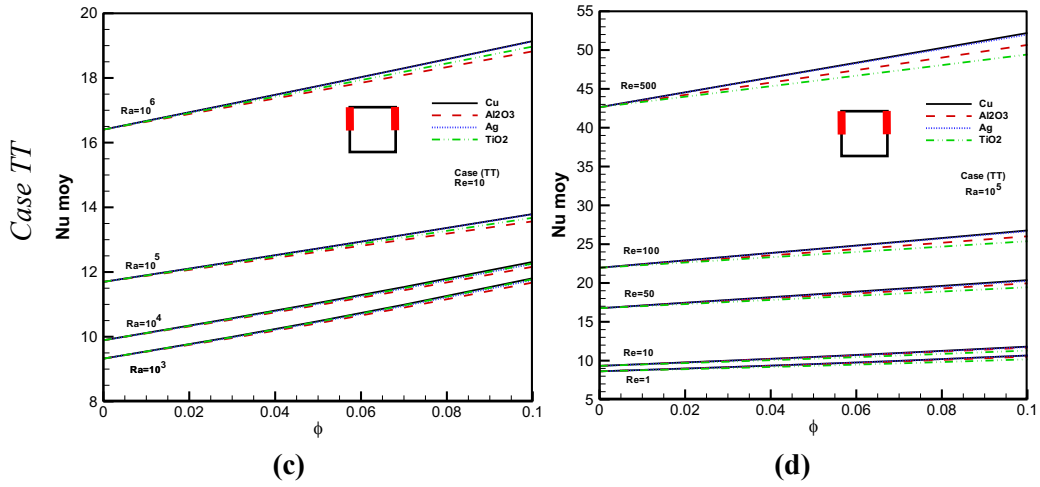
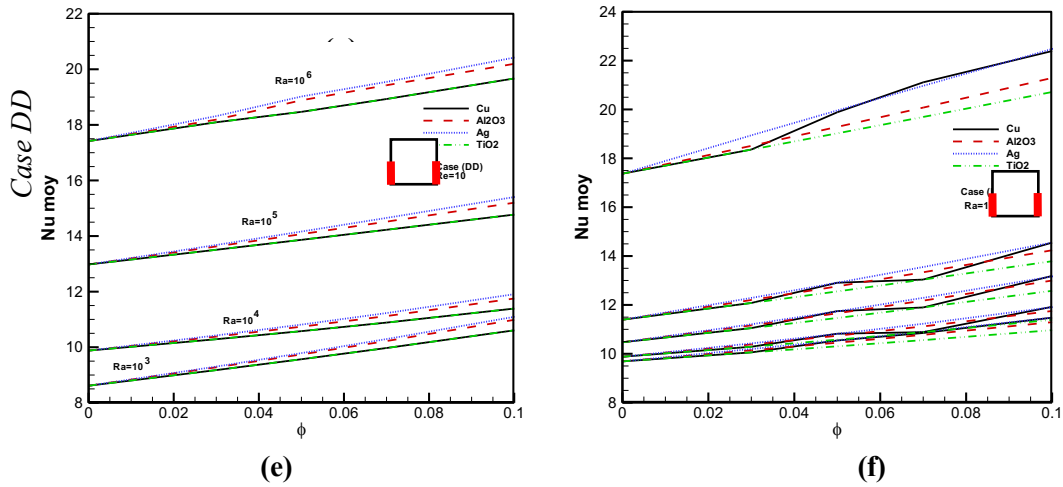


Figure 6: Variation of average Nusselt number Nu_m along the heat source with solid volume fraction at various Rayleigh and Reynolds numbers and different nanofluids for: (a) and (b) MM case, (c) and (d) TT case, (e) and (f) DD case, (g) and (h) TD case



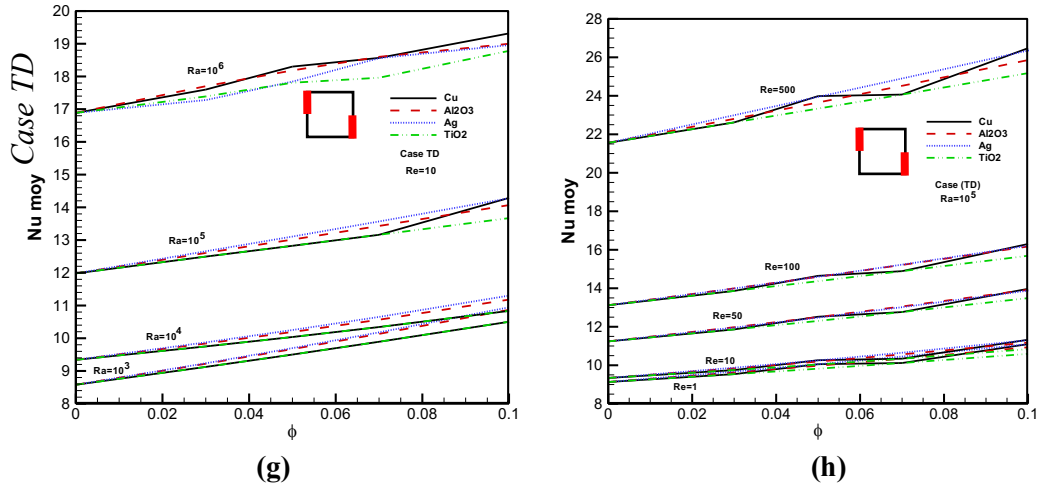
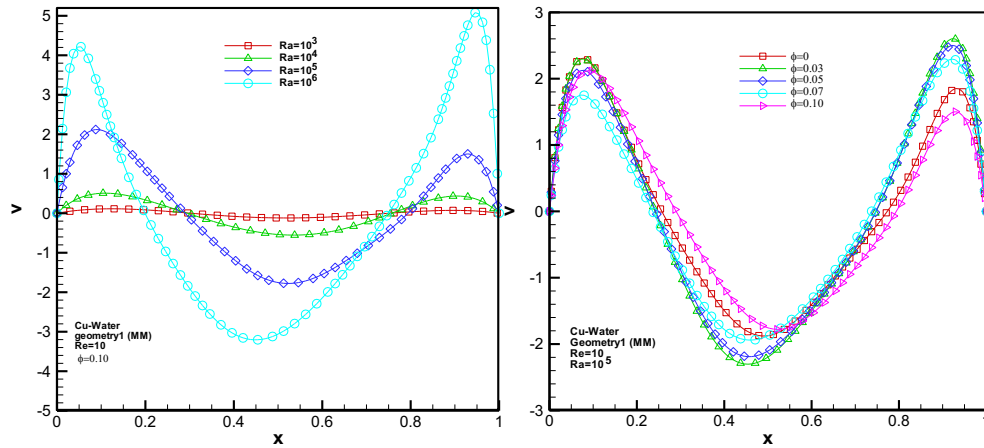


Figure 6 (continued)

4.4 Effects of Rayleigh number, solid volume fraction and Reynolds number on the vertical velocity and local Nusselt number

Figures 7 show the effect of Rayleigh and Reynolds numbers and solid volume fraction on the vertical velocity V at the midsection of the cavity for MM case and Cu-water nanofluid. We can clearly see that the vertical component of the velocity increases with increase in Rayleigh, while it decreases when the volume concentration of nanofluid increases ($\phi=0\div 0.10$), and for the Reynolds number.



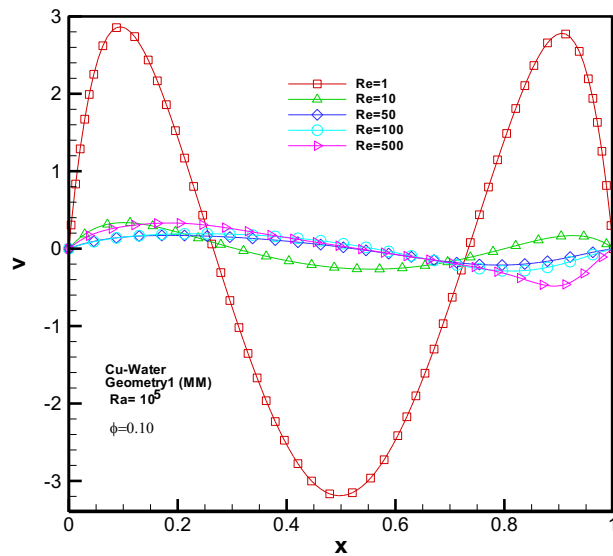
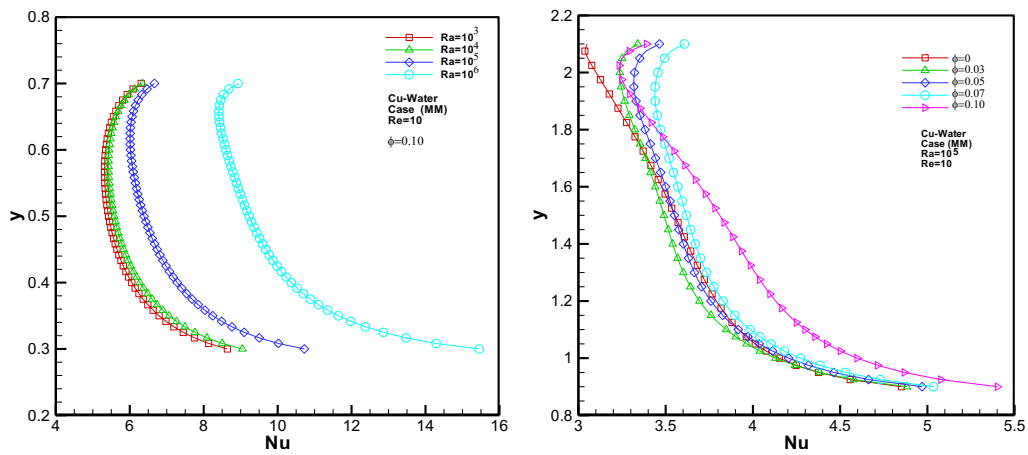


Figure 7: Effect of Rayleigh Ra and Reynolds Re numbers and solid volume fraction ϕ on the vertical velocity V component at the mid-section of the cavity (MM case and Cu-water nanofluid)



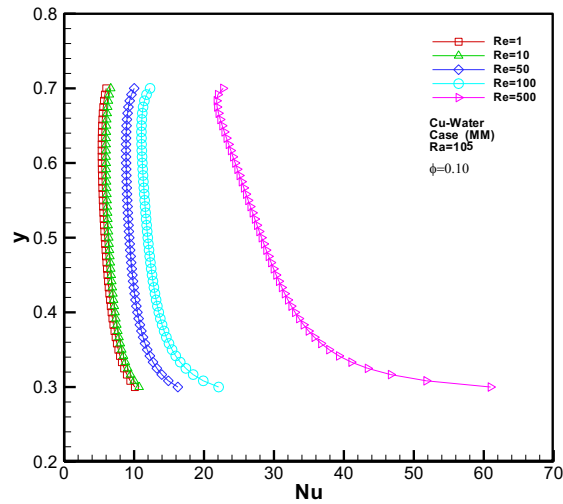


Figure 8: Effect of Rayleigh Ra and Reynolds Re numbers and solid volume fraction ϕ on the local Nusselt number Nu along the heat source (MM case and Cu-water nanofluid)

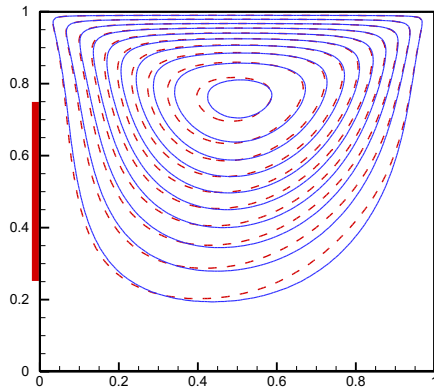
Figure 8 displays the effect of Rayleigh and Reynolds numbers and solid volume fraction on the local Nusselt number Nu along the heat source for MM case and Cu-water nanofluid. It was found that the local Nusselt number along both heating elements becomes important when an increase is recorded on the Rayleigh number, the Reynolds number and the volume fraction of nanofluid. The local Nusselt number reaches values $Nu=14.8$, 12.5 and 63 . This result demonstrates the positive role of the Rayleigh number when it is important in increasing the transfer rate by increasing the local Nusselt number along the heat sources, and the increasing speed obtained near the heating walls against by the Reynolds number. The symmetry between the upflow and downflow from the centre of the cavity has been reported in the outcomes studied. Also, it was noted that the increasing volume concentration of copper particles in the nanofluid acted positively on the vertical velocity component. This is mainly due to the gravity of the nanofluid, because the fluid becomes heavy when is increasingly loaded nanoparticles, resulting a difficult and cumbersome movement of the copper particles to the upper part of the cavity. Salari et al. [Salari, Tabar, Tabar et al. (2012)] confirmed these results, in their study of partially cooling a heated mixed convection mode cavity. As confirmed by Mansour et al. [Mansour, Galanis and Nguyen (2011)], in their study of the joint in a convection chamber provided with a heat source at the bottom of the cavity.

4.5 Effects of heat sources position

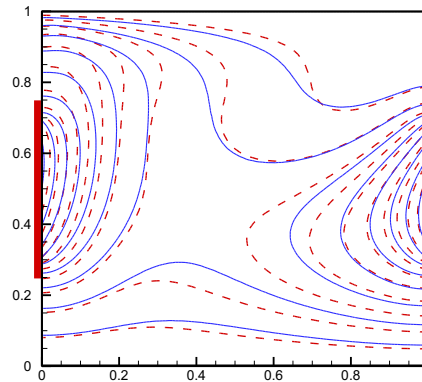
Figure 9 illustrates the streamlines (on the left) and isotherms (on the right) for different values of Reynolds number for the lid-driven cavities filled with Cu-water nanofluid $\phi=0.1$. Our study is based on four configurations in which several locations of heat sources have been studied numerically. In all four configurations, we have seen the generation of a recirculation zone within the cavity in approaching any active top wall. The intensity of the flow becomes more pronounced, this was observed in both (TT) and (TD) cases, so the streamlines become significant when two heat sources are close to the sliding wall. This is due essentially the movement of the wall and around the area, for against the other two

locations (MM) and (DD) cases streamlines are quieter. For (MM) case, it is interesting to note that the dimensionless maximum temperature is reached for both heat sources attached to the midsection of the cavity.

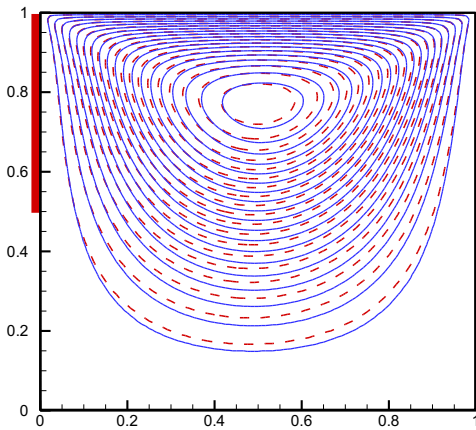
Finally, we can conclude that the location of heat sources significantly affects the heat transfer, and the perfect configuration that can ensure proper cooling of the cavity is that of the (TT) case near the movable wall.



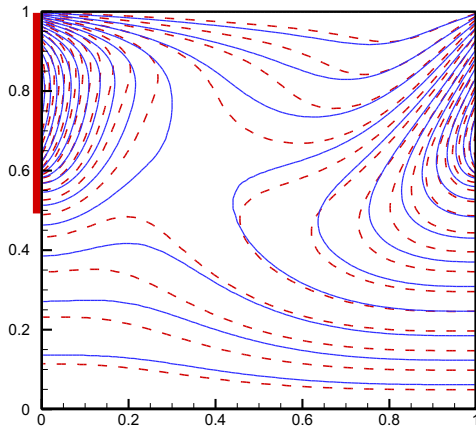
(a) $\Psi_{\min,f} = -0.1044$ $\Psi_{\max,f} = 0.0006$
 $\Psi_{\min,nf} = -0.1032$ $\Psi_{\max,nf} = 0.0001$



(b) $\theta_{\max,l,f} = 0$ $\theta_{\max,r,f} = 0.2257$
 $\theta_{\max,l,nf} = 0$ $\theta_{\max,r,nf} = 0.1843$



(c) $\Psi_{\min,f} = -0.0982$ $\Psi_{\max,f} = 0$
 $\Psi_{\min,nf} = -0.0989$ $\Psi_{\max,nf} = 0$



(d) $\theta_{\max,l,f} = 0$ $\theta_{\max,r,f} = 0.1776$
 $\theta_{\max,l,nf} = 0$ $\theta_{\max,r,nf} = 0.1449$

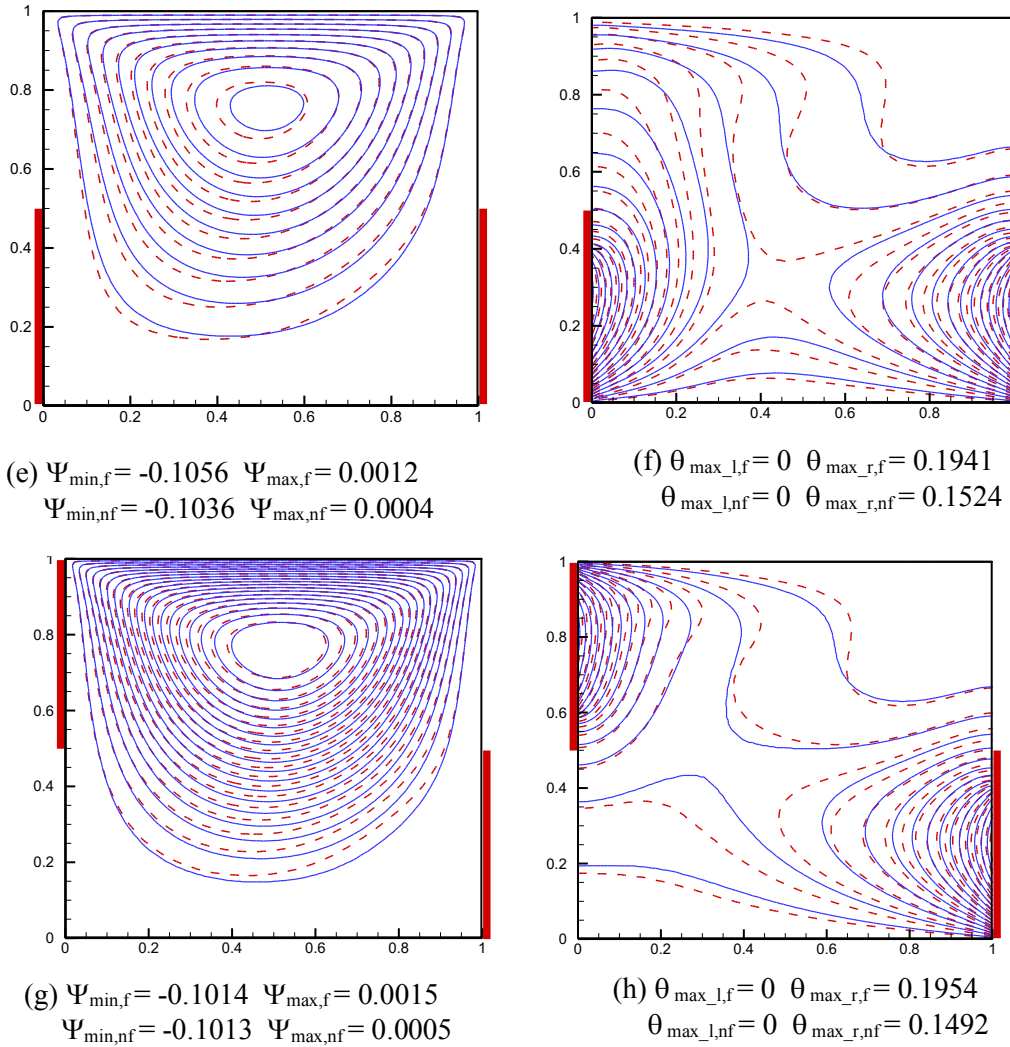


Figure 9: Streamlines (on the left) and isotherms (on the right) for different values of Reynolds number for the lid-driven cavities filled with Cu-water nanofluid, $\phi=0.10$ (---), and pure water $\phi=0$ (—) at $Ra=10^4$ and $Re=10$ for various cases: (a) and (b) MM case, (c) and (d) TT case, (e) and (f) DD case, (g) and (h) TD case

5 Conclusion

A numerical study of two-dimensional laminar mixed convection in a lid-driven square cavity filled with a nanofluid and heated simultaneously at a constant heat flux by two heat sources placed on the two vertical walls was carried out. The finite volume method was used to solve the mathematical equations. A comparison with previously published work was performed and the results were to be in good agreement. The results show that the

effect of previous parameters has considerable effects on the flow and heat transfer. The important concluding remarks are presented below:

- Increasing the Rayleigh number, the maximum dimensionless temperature decreases and the intensity of the flow increases through the increase of streamlines, and the average Nusselt number increases along the heat sources.
- Increasing the Reynolds number, the movable cover increases due to forced convection, and the maximum temperature decreases.
- The type of nanofluids and the heat sources location inside the cavity greatly affect the variation of the average Nusselt number.
- The top-top (TT) configuration ensures proper cooling of the cavity.
- Increasing the concentration of the nanofluid decreases the vertical velocity and increases the local Nusselt number.

References

Abu-Nada, E.; Chamkha, A. J. (2010): Mixed convection flow in a lid-driven inclined square enclosure filled with a nanofluid. *European Journal of Mechanics-B/Fluids*, vol. 29, pp. 472-482.

Akbari, M.; Behzadmehr, A.; Shahraki, F. (2008): Fully developed mixed convection in horizontal and inclined tubes with uniform heat flux using nanofluid. *International Journal of Heat and Fluid Flow*, vol. 29, pp. 545-556.

Akbarinia, A.; Behzadmehr, A. (2007): Numerical study of laminar mixed convection of a nanofluid in horizontal curved tubes. *Applied Thermal Engineering*, vol. 27, pp. 1327-1337.

Alinia, M.; Ganji, D. D.; Gorji-Bandpy, M. (2011): Numerical study of mixed convection in an inclined two-sided lid-driven Ccavity filled with nanofluid using two-phase mixture model. *International Communications in Heat and Mass Transfer*, vol. 38, pp. 1428-1435.

Arami, A. A.; Sebdani, S. M.; Mahmoudi, M. (2012): Numerical study of mixed convection flow in a lid-driven cavity with sinusoidal heating on sidewalls using nanofluid. *Superlattices and Microstructures*, vol. 51, pp. 893-911.

Brinkman, H. C. (1952): The viscosity of concentrated suspensions and solution. *Journal of Physical Chemistry*, vol. 20, pp. 571-581.

Choi, U. S. (1995): Enhancing thermal conductivity of fluids with nanoparticles. *ASME Fluids Engineering Division Summer Meeting*, vol. 231, pp. 99-105.

Haddad, Z.; Oztop, H. F.; Abu-Nada, E.; Mataoui, A. (2012): A Review on natural convective heat transfer of nanofluids. *Renewable and Sustainable Energy Reviews*, vol. 16, pp. 5363-5378.

Jmai, R.; Ben-Beya, B.; Lili, T. (2013): Heat transfer and fluid flow of nanofluid-filled enclosure with two partially heated sidewalls and different nanoparticles. *Superlattices and Microstructures*, vol. 53, pp.130-154.

Khorasanizadeh, H.; Nikfar, M.; Amani, J. (2013): Entropic generation of cu-water nanofluid mixed convection in a cavity. *European Journal of Mechanics-B/Fluids*, vol. 37, pp. 143-152.

Mahmoudi, A. H.; Shahi, M.; Shahedin, A. M.; Hemati, N. (2011): Numerical modeling of natural convection in an open cavity with two vertical thin heat sources subjected to a nanofluid. *International Communications in Heat and Mass Transfer*, vol. 38, pp. 110-118.

Mahmoudi, A. H.; Shahi, M.; Talebi, F. (2010): Effect on inlet and outlet location on the mixed convection cooling inside the ventiled cavity subjected to an external nanofluid. *International Communications in Heat and Mass Transfer*, vol. 37, pp. 1158-1173.

Mahmoudi, M. (2011): Numerical simulation of free convection of nanofluid in a square cavity with an inside heater. *International Journal of Thermal Sciences*, vol. 50, pp. 2161-2175.

Mahmoudi, M.; Hashemi, S. M. (2012): Numerical study of natural convection of a nanofluid in C-shaped enclosures. *International Journal of Thermal Sciences*, vol. 55, pp. 76-89.

Mahmoudi, M.; Sebdani, S. M. (2012): Natural convection in a square block at the center. *Superlattices and Microstructures*, vol. 52, pp. 261-275.

Mansour, M. A.; Mohamed, R. A.; Abdel-Elaziz, M. M.; Ahmed, S. E. (2010): Numerical simulation of mixed convection flows in a square lid-driven cavity partially heated from below using nanofluid. *International Communications in Heat and Mass Transfer*, vol. 37, pp. 1504-1512.

Mansour, R. B.; Galanis, N.; Nguyen, C. T. (2011): Experimental study of mixed convection with water Al_2O_3 nanofluid in inclined tube with uniform wall heat flux. *International Journal of Thermal Sciences*, vol. 50, pp. 403-410.

Nasrin, R.; Alim, M. A.; Chamkha, A. J. (2012): Combined convection flow in triangular wavy chamber filled with water-Cu nanofluid: Effect of viscosity models. *International Communications in Heat and Mass Transfer*, vol. 39, pp. 1226-1236.

Patankar, S. V. (1980): *Numerical heat transfer and fluid Flow*. Hemisphere, Washington, DC.

Pishkar, I.; Ghasemi, B. (2012): Cooling enhancement of two fins in a horizontal channel by nanofluid mixed convection. *International Journal of Thermal Sciences*, vol. 59, pp. 141-151.

Pourmahmoud, N.; Ghafouri, A.; Mirzall, I. (2013): Numerical study of mixed convection heat transfer in lid-driven cavity utilizing nanofluid: Effect of type and model. *Thermal Science*, vol. 53-53.

Rahman, M. M.; Billah, M. M.; Hasanezzaman, M.; Saidur, R. N. A. (2012): Heat transfer enhancement of nanofluid in a lid-driven square enclosure. *Numerical Heat Transfer, Part A*, vol. 62, pp. 973-991.

Salari, M.; Tabar, M. M.; Tabar, A. M.; Danesh, H. A. (2012): Mixed convection of nanofluid flows in a square lid-driven cavity heated partially from both the bottom and side walls. *Numerical Heat Transfer, Part A*, vol. 62, pp. 158-177.

Sebdania, S. M.; Mahmoodia, M.; Hashemi, S. M. (2012): Effect of nanofluid variable properties on mixed convection in a square cavity. *International Journal of Thermal Sciences*, vol. 52, pp. 112-126.

Shahi, M.; Mahmoudi, A. H.; Talebi, F. (2010): Numerical study of mixed convection cooling in a square cavity ventilated and partially heated from the below utilizing nanofluid. *International Communications in Heat and Mass Transfer*, vol. 37, pp. 201-213.

Shariat, M.; Akbarinia, A.; Nezhad, A. H.; Behzadmehr, A. (2011): Numerical study of two phase laminar mixed convection nanofluid in elliptic ducts. *Applied Thermal Engineering*, vol. 31, pp. 2348-2359.

Soleimani, S.; Oleslani, M. S.; Ganji, D. D.; Bandpay, M. G. (2012): Natural convection heat transfer in a nanofluid filled semi-annulus enclosure. *International Communications in Heat and Mass Transfer*, vol. 39, pp. 565-574.

Talebi, F.; Mahmoudi, A. H.; Shahi, M. (2010): Numerical study of mixed convection flows in a square lid-driven cavity utilizing nanofluid. *International Communications in Heat and Mass Transfer*, vol. 37, pp. 79-90.